Phased breaking of $\mu - \tau$ symmetry and leptogenesis

Y. H. Ahn,[1,*] Sin Kyu Kang,[2,†] C. S. Kim,[1,‡] and Jake Lee[2,§]

[1]*Department of Physics, Yonsei University, Seoul 120-749, Korea*
[2]*Center for Quantum Spacetime, Sogang University, Seoul 121-742, Korea*
(Received 10 March 2006; published 19 May 2006)

Nonvanishing U_{e3} has been theoretically related to a certain flavor symmetry breaking in the neutrino sector. We propose a scenario to break the $\mu - \tau$ symmetry so as to accommodate the nonvanishing U_{e3}. Our scenario is constructed in the context of a seesaw model, and the $\mu - \tau$ symmetry breaking is achieved by introducing a *CP* phase in the Dirac Yukawa matrix. We also show how the deviation of θ_{23} from the maximal mixing and nonvanishing U_{e3} depend on the *CP* phase. Neutrino mixings and the neutrino mass-squared differences are discussed, and the amplitude in neutrinoless double beta decay m_{ee} are also predicted. We found that a tiny breaking of the $\mu - \tau$ symmetry due to mass splitting between two degenerate heavy Majorana neutrinos on top of the Dirac *CP* phase can lead to successful leptogenesis. We examine how leptogenesis can be related with low energy neutrino measurement, and show that our predictions for U_{e3} and m_{ee} can be constrained by the current observation of baryon asymmetry.

DOI: 10.1103/PhysRevD.73.093005 PACS numbers: 14.60.Pq, 11.30.Fs, 13.35.Hb, 98.80.Cq

I. INTRODUCTION

Thanks to the recent precise neutrino experiments, we now have robust evidences for the neutrino oscillation. The present neutrino experimental data [1–3] indicate that the atmospheric neutrino deficit points toward a maximal mixing between the tau and muon neutrinos, however the solar neutrino deficit favors a not-so-maximal mixing between the electron and muon neutrinos. In addition, although we do not have yet any evidence for the neutrino oscillation arisen from the 1st and 3rd generation flavor mixing, there is a bound on the mixing element U_{e3} from CHOOZ reactor experiment, $|U_{e3}| < 0.2$ [4]. Although neutrinos have gradually revealed their properties in various experiments since the historic Super-Kamiokande confirmation of neutrino oscillations [1], properties related to the leptonic *CP* violation are completely unknown yet. To understand in detail the neutrino mixings observed in various oscillation experiments is one of the most interesting puzzle in particle physics. The large value of $\theta_{\rm sol}$ and $\theta_{\rm atm}$ may be telling us about some new symmetries of leptons that are not present in the quark sector and may provide a clue to understanding the nature of quark-lepton physics beyond the standard model.

Recently, there have been some attempt to explain the maximal mixing of the atmospheric neutrinos and very tiny value of the 3rd mixing element U_{e3} by introducing some approximate discrete symmetries [5,6] or the mass splitting among the heavy Majorana neutrinos in the seesaw framework [7]. In the basis where charged leptons are mass eigenstates, the $\mu - \tau$ interchange symmetry has become useful in understanding the maximal atmospheric neutrino mixing and the smallness of U_{e3} [8–11]. The mass difference between the muon and the tau leptons, of course, breaks this symmetry in the basis. So we expect this symmetry to be an approximate one, and thus it must hold only for the neutrino sector at low energy.

On the other hand, finding nonvanishing but small mixing element U_{e3} would be very interesting in the sense that the element is closely related to leptonic *CP* violation [12]. If future neutrino experiments would measure the nonvanishing U_{e3} [13], it may indicate from the aforementioned point of view that the $\mu - \tau$ symmetry must be broken. Motivated by this prospect, in this paper, we propose a scenario to break the $\mu - \tau$ symmetry so as to accommodate the nonvanishing U_{e3}. Our scenario is constructed in the context of a seesaw model, and the symmetry breaking is first achieved by introducing a *CP* phase in the Dirac Yukawa matrix. Then, the resultant effective light neutrino mass matrix generated through seesaw mechanism reflects the $\mu - \tau$ symmetry breaking, which is parameterized in terms of the *CP* phase. The $\mu - \tau$ symmetry should be recovered in the limit of vanishing *CP* phase.

In fact, the breaking of the $\mu - \tau$ symmetry through a *CP* phase has been also discussed in Ref. [14], in which the authors have studied the breaking in the framework of the effective light neutrino mass matrix. In Ref. [11] the breaking has been also achieved through the heavy Majorana neutrino mass matrix with complex elements, which is completely different from our scheme. We will study how neutrino mixings and the neutrino mass-squared difference can be predicted and show how the deviation of θ_{23} from the maximal mixing and nonvanishing U_{e3} depend on the *CP* phase in our scenario. The prediction for the amplitude in neutrinoless double beta decay will be discussed as well. However, it is turned out that the Dirac *CP*

*Electronic address: yhahn@cskim.yonsei.ac.kr
†Electronic address: skkang1@sogang.ac.kr
‡Electronic address: cskim@yonsei.ac.kr
§Electronic address: jilee@cskim.yonsei.ac.kr

phase introduced to break the $\mu - \tau$ symmetry does not lead to successful leptogenesis, and thus we need a subsidiary source for the lepton asymmetry. We will show that a tiny breaking of the degeneracy between two heavy Majorana neutrinos, in addition, can lead to successful leptogenesis without much affecting the predictions of the low energy neutrino observables. We will also examine how leptogenesis can be related with low energy neutrino measurement, and show that our predictions for U_{e3} and m_{ee} can be constrained by the current observation of baryon asymmetry.

II. NEUTRINO SECTORS WITH $\mu - \tau$ SYMMETRY

To begin with, let us consider the Lagrangian of the lepton sector from which the seesaw mechanism works,

$$\mathcal{L}_m = -Y_\nu^{ik}\bar{L}_i N_k \tilde{\phi} - Y_l^i \bar{L}_i l_{R_i} \phi - \frac{1}{2}\bar{N}_k^c M_{N_k} N_k + \text{H.}c., \quad (1)$$

where $i = e, \mu, \tau$ and $k = 1, 2, 3$. L_i, l_R, ϕ, N are $SU(2)$ lepton doublet fields, charged lepton singlet fields and Higgs scalar, singlet heavy Majorana neutrino, respectively, and M_{N_k} denotes heavy Majorana neutrino masses. Here we take a basis in which both charged lepton and singlet Majorana neutrino mass matrices are real and diagonal. The neutrino Dirac Yukawa matrix with $\mu - \tau$ symmetry is given in the CP conserving limit by

$$Y_\nu = \begin{pmatrix} a & b & b \\ b & c & d \\ b & d & c \end{pmatrix}, \quad (2)$$

where we assumed that Y_ν is symmetric. The Majorana mass matrix M_N with $\mu - \tau$ symmetry is given in the diagonal form by $M_N = \text{Diag}[M_1, M_2, M_2]$. Note the degeneracy of $M_2 = M_3$ from the presumed $\mu - \tau$ symmetry. Later we will discuss the effects of breaking the mass degeneracy, too. Then, the effective light neutrino mass matrix generated through seesaw mechanism reflects $\mu - \tau$ symmetry which in turn leads to maximal mixing of the atmospheric neutrinos and vanishing mixing angle θ_{13} in PMNS mixing matrix. In order to obtain nonvanishing θ_{13}, we have to break $\mu - \tau$ symmetry appropriately. The $\mu - \tau$ symmetry breaking can generally be achieved by imposing splittings between the same entries in the mass matrices Y_ν and M_N. In this paper, however, we break the symmetry by introducing a CP phase in the Dirac Yukawa matrix Y_ν so that the same entries are distinguishable by the phase. In principle, we can arbitrarily introduce CP phases in the above Dirac Yukawa matrix to break the symmetry. However, we note that any phases appearing in (2) and (3) submatrix of the effective light neutrino mass matrix should be small to satisfy the experimental result of $\Delta m^2_{\text{sol}}/\Delta m^2_{\text{atm}}$ [14]. In this regard, it is relevant to impose CP phases in (1) and (2) and/or (1) and (3) entries of the Dirac Yukawa matrix while keeping any entries in (2) and (3) submatrix of the effective light neutrino mass matrix real. For simplicity, we take the (1) and (3) entry to include a CP phase. Actually, either choice is turned out to be completely equivalent. Incorporating a CP phase in (1) and (3) entry of the Dirac mass matrix, the effective light neutrino mass matrix through seesaw mechanism is given by

$$\begin{aligned} m_{\text{eff}} &= -v^2 Y_\nu^T M_N^{-1} Y_\nu \\ &= -v^2 \begin{pmatrix} a & b & b \\ b & c & d \\ be^{i\alpha} & d & c \end{pmatrix}^T \begin{pmatrix} M_1 & 0 & 0 \\ 0 & M_2 & 0 \\ 0 & 0 & M_2 \end{pmatrix}^{-1} \begin{pmatrix} a & b & b \\ b & c & d \\ be^{i\alpha} & d & c \end{pmatrix} \\ &= -v^2 \begin{pmatrix} \frac{a^2}{M_1} + \frac{b^2(1+e^{2i\alpha})}{M_2} & \frac{ab}{M_1} + \frac{b(c+de^{i\alpha})}{M_2} & \frac{ab}{M_1} + \frac{b(d+ce^{i\alpha})}{M_2} \\ \frac{ab}{M_1} + \frac{b(c+de^{i\alpha})}{M_2} & \frac{b^2}{M_1} + \frac{c^2+d^2}{M_2} & \frac{b^2}{M_1} + \frac{2cd}{M_2} \\ \frac{ab}{M_1} + \frac{b(d+ce^{i\alpha})}{M_2} & \frac{b^2}{M_1} + \frac{2cd}{M_2} & \frac{b^2}{M_1} + \frac{c^2+d^2}{M_2} \end{pmatrix}. \end{aligned} \quad (3)$$

As one can easily see, the nontrivial value of the CP phase α in the mass matrix m_{eff} breaks the $\mu - \tau$ symmetry.

III. NEUTRINO MIXING ANGLES, A DIRAC CP PHASE AND NEUTRINO MASS SPECTRUM

First, we consider how the neutrino mixing angles and neutrino mass spectrum can be predicted in our scenario. As can be expected from the structure of the above m_{eff}, in our model only the normal hierarchical mass spectrum is allowed because the inverted hierarchical case is achieved only when the off-diagonal elements in heavy Majorana neutrino mass matrix are dominant [15], which is in contrast with the case of our model. Furthermore, considering the normal hierarchy and the maximality of the atmospheric neutrino mixing, one can expect the following hierarchical structure among the elements of the effective light neutrino mass matrix:

$$|m_{\mu\tau,\mu\mu,\tau\tau}| \gg |m_{e\mu,e\tau}| \gg |m_{ee}|. \quad (4)$$

In terms of the light neutrino mass eigenvalues m_i, the above condition (4) leads to

$$\begin{aligned} |m_3| &\simeq |(m_{\text{eff}})_{22} - (m_{\text{eff}})_{23}| \gg |m_2| \\ &\simeq |(m_{\text{eff}})_{22} + (m_{\text{eff}})_{23}|, \end{aligned}$$

and then we get the following relations in terms of our parameters appeared in Eq. (3):

$$\frac{2|cd|}{M_2} \gg \frac{b^2}{M_1}, \qquad cd < 0, \quad (5)$$

$$|a| \ll |b| \ll |c| \sim |d|, \quad (6)$$

where the degree of the hierarchy in Eq. (6) will depend on that of the heavy Majorana masses M_1 and M_2. Introducing new parameters from the ratios among the parameters given in Eq. (3),

$$m_0 \equiv v^2 \frac{d^2}{M_2}, \qquad \eta \equiv \frac{M_1}{M_2}, \qquad \rho \equiv \frac{a}{d}, \qquad \omega \equiv \frac{b}{d}, \qquad \kappa \equiv \frac{c}{d}, \tag{7}$$

we can reparametrize the neutrino mass matrix m_{eff} as follows:

$$m_{\text{eff}} = m_0 \begin{pmatrix} \frac{\rho^2}{\eta} + (e^{2i\alpha} + 1)\omega^2 & \frac{\rho\omega}{\eta} + (\kappa + e^{i\alpha})\omega & \frac{\rho\omega}{\eta} + (1 + \kappa e^{i\alpha})\omega \\ \frac{\rho\omega}{\eta} + (\kappa + e^{i\alpha})\omega & \frac{\omega^2}{\eta} + 1 + \kappa^2 & \frac{\omega^2}{\eta} + 2\kappa \\ \frac{\rho\omega}{\eta} + (1 + \kappa e^{i\alpha})\omega & \frac{\omega^2}{\eta} + 2\kappa & \frac{\omega^2}{\eta} + 1 + \kappa^2 \end{pmatrix}. \tag{8}$$

Depending on the hierarchy of the heavy Majorana neutrino masses M_1 and M_2, the relative sizes of the new parameters consistent with the normal hierarchy of the neutrino mass spectrum and the hierarchy of Δm^2_{sol} and Δm^2_{atm} can be classified as follows:

$$\begin{aligned} &\text{case 1}(M_2 \gg M_1)\text{: } 1 \gg \eta \sim |\kappa|\eta \gg \omega \\ &\qquad\qquad \text{or} \quad 1 \gg \omega \gg \eta|\kappa| \sim \eta \gg \eta\omega, \\ &\text{case 2}(M_2 \simeq M_1)\text{: } 1 \sim \eta \sim |\kappa|\eta \gg \omega, \\ &\text{case 3}(M_2 \ll M_1)\text{: } \eta \gg |\kappa| \gg \omega. \end{aligned} \tag{9}$$

Note that κ is negative as can be seen in the relation (5), and the quantity ρ/η is very small compared to the other ones in m_{eff}. For numerical purpose, we consider the case of $\rho = 0$ without a loss of generality. Then the neutrino mass matrix m_{eff} is simplified as

$$\begin{aligned} m_{\text{eff}} &= m_0 \begin{pmatrix} (e^{2i\alpha} + 1)\omega^2 & (\kappa + e^{i\alpha})\omega & (1 + \kappa e^{i\alpha})\omega \\ (\kappa + e^{i\alpha})\omega & \frac{\omega^2}{\eta} + 1 + \kappa^2 & \frac{\omega^2}{\eta} + 2\kappa \\ (1 + \kappa e^{i\alpha})\omega & \frac{\omega^2}{\eta} + 2\kappa & \frac{\omega^2}{\eta} + 1 + \kappa^2 \end{pmatrix} \\ &\equiv \begin{pmatrix} \tilde{p} & \tilde{q} & \tilde{q}' \\ \tilde{q} & r & s \\ \tilde{q}' & s & r \end{pmatrix}, \end{aligned} \tag{10}$$

where the complex variables are distinguished by the tilde. This neutrino mass matrix is diagonalized by the PMNS mixing matrix U_{PMNS}, $U^T_{\text{PMNS}} m_{\text{eff}} U_{\text{PMNS}} = \text{Diag}[m_1, m_2, m_3]$, where $m_i (i = 1, 2, 3)$ indicates the mass eigenvalues of light Majorana neutrinos. But, we diagonalize the hermitian matrix $m^\dagger_{\text{eff}} m_{\text{eff}}$ [16,17] instead, so that we can easily obtain the mixing angles and phases appeared in U_{PMNS} in terms of the parameters appeared in Eq. (10),

$$\begin{aligned} m^\dagger_{\text{eff}} m_{\text{eff}} &= U_{\text{PMNS}} \text{Diag}(m_1^2, m_2^2, m_3^2) U^\dagger_{\text{PMNS}} \\ &\equiv \begin{pmatrix} A & \tilde{B} & \tilde{C} \\ \tilde{B}^* & D & \tilde{E} \\ \tilde{C}^* & \tilde{E}^* & D \end{pmatrix}, \end{aligned} \tag{11}$$

where

$$\begin{aligned} &A = |\tilde{p}|^2 + |\tilde{q}|^2 + |\tilde{q}'|^2, \qquad \tilde{B} = \tilde{p}^*\tilde{q} + \tilde{q}^* r + \tilde{q}'^* s, \\ &\tilde{C} = \tilde{p}^*\tilde{q}' + \tilde{q}^* s + \tilde{q}'^* r, \qquad D = |\tilde{q}|^2 + r^2 + s^2, \\ &\qquad\qquad \tilde{E} = \tilde{q}^*\tilde{q}' + 2rs. \end{aligned} \tag{12}$$

Here we note that A and D are real. Then, the straightforward calculation with the standard parametrization of U_{PMNS} leads to the expressions for the masses and mixing parameters [17]:

$$\begin{aligned} m^2_{1,2} &= \frac{\lambda_1 + \lambda_2}{2} \mp \frac{c_{23}\,\text{Re}(\tilde{B}) - s_{23}\,\text{Re}(\tilde{C})}{2 s_{12} c_{12} c_{13}}, \\ m^2_3 &= \frac{c^2_{13}\lambda_3 - s^2_{13} A}{c^2_{13} - s^2_{13}}, \end{aligned} \tag{13}$$

$$\begin{aligned} &\tan\theta_{23} = \frac{\text{Im}(\tilde{B})}{\text{Im}(\tilde{C})}, \qquad \tan 2\theta_{12} = 2\frac{c_{23}\,\text{Re}(\tilde{B}) - s_{23}\,\text{Re}(\tilde{C})}{c_{13}(\lambda_2 - \lambda_1)}, \\ &\qquad \tan 2\theta_{13} = 2\frac{|s_{23}\tilde{B} + c_{23}\tilde{C}|}{\lambda_3 - A}, \end{aligned} \tag{14}$$

$$\tan\delta = -\frac{1}{s_{23}} \frac{\text{Im}(\tilde{B})}{s_{23}\,\text{Re}(\tilde{B}) + c_{23}\,\text{Re}(\tilde{C})}, \tag{15}$$

with

$$\begin{aligned} \lambda_1 &= c^2_{13} A - 2 s_{13} c_{13} |s_{23}\tilde{B} + c_{23}\tilde{C}| + s^2_{13}\lambda_3, \\ \lambda_{2,3} &= D \mp 2 s_{23} c_{23}\,\text{Re}(\tilde{E}). \end{aligned} \tag{16}$$

As can be seen from Eqs. (10)–(16), three neutrino masses, three mixing angles and a CP phase are presented in terms of five independent parameters m_0, ω, κ, η, α. At present, we have five experimental results, which are taken as inputs in our numerical analysis given at 3σ by [18],

$$\begin{aligned} &28.7° < \theta_{12} < 38.1°, \qquad 35.7° < \theta_{23} < 55.6°, \\ &0° < \theta_{13} < 13.1°, \qquad 7.1 < \Delta m^2_{21}[10^{-5}\ \text{eV}^2] < 8.9, \\ &\qquad 1.4 < \Delta m^2_{31}[10^{-3}\ \text{eV}^2] < 3.3. \end{aligned} \tag{17}$$

Imposing the current experimental results on neutrino masses and mixings into the above relations (13)–(16) and scanning all the parameter space m_0, ω, κ, η, α, we investigate how those parameters are constrained and estimate possible predictions for other phenomena such as neutrinoless double beta decay and leptonic CP violation.

Let us discuss the numerical results focusing on the three cases given in (9). As a result of the numerical analysis concerned with the mixing angle θ_{12}, we found that the Case 1 ($M_2 \gg M_1$) is ruled out mainly because we get a very small θ_{12} for all the parameter space in this case. So, we will focus on Case 2 and Case 3. In Fig. 1, we show the parameter regions constrained by the experimental results given in Eq. (17) for $\eta = 1$. The two figures present how the parameter κ can be constrained depending on the parameter ω and the phase α, respectively. The allowed range of m_0 is turned out to be $10^{-3} \sim 10^{-2}$ eV. In Fig. 2, we show the same constrained parameter regions for Case 3. Here we fix $\eta = 1000$, however, we found that the dependence of η on the allowed regions of the other parameters is very weak as long as $\eta \geq 10$.

We note that the most severe constraint for the parameters comes from the solar mixing angle θ_{12}. To see how the solar mixing angle constrain the parameters, it is useful to consider the approximate form of θ_{12} in the limit of maximal θ_{23} and tiny θ_{13}, which is given by

$$\tan 2\theta_{12} \simeq \frac{2\sqrt{2}(1+\kappa)\omega\cos^2\frac{\alpha}{2}\{(1+\kappa)^2 + 2\frac{\omega^2}{\eta} + 2\omega^2\cos\alpha\}}{(1+\kappa)^4 + (\kappa-1)^2\omega^2(\cos\alpha - 1) + 4(1+\kappa)^2\frac{\omega^2}{\eta} + 4\frac{\omega^4}{\eta^2}}. \quad (18)$$

Based on the above expression, let us discuss the predictions of the mixing angle θ_{12} case by case classified in (9).

(i) For Case 2, the solar mixing angle is further approximated:

$$\tan 2\theta_{12} \simeq \frac{2\sqrt{2}(1+\kappa)\omega\cos^2\frac{\alpha}{2}\{(1+\kappa)^2 + 2\omega^2(1+\cos\alpha)\}}{(1+\kappa)^4 + (\kappa-1)^2\omega^2(\cos\alpha - 1) + 4\omega^2\{(1+\kappa)^2 + \omega^2\}}. \quad (19)$$

As can be seen in Fig. 1, the current experimental values of θ_{12} are achieved only when the condition $|1+\kappa| \sim |\omega|$

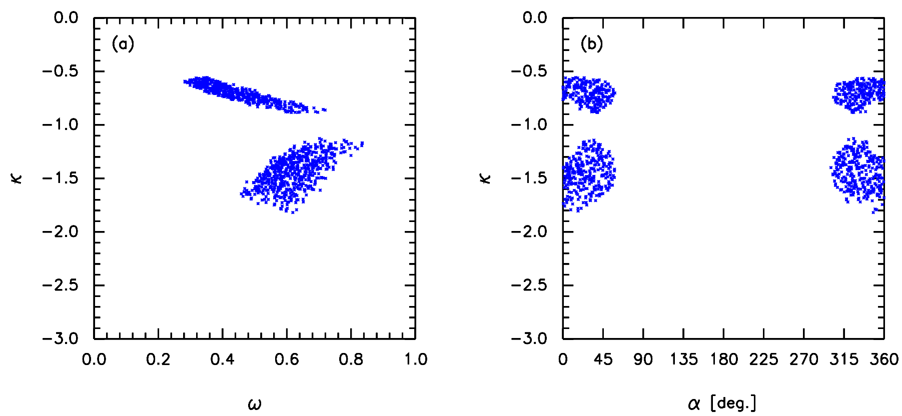

FIG. 1 (color online). Allowed parameter regions by the 3σ experimental constraints in Eq. (17) of Case 2 ($M_2 \simeq M_1$) in Eq. (9). Here we take $\eta = 1$.

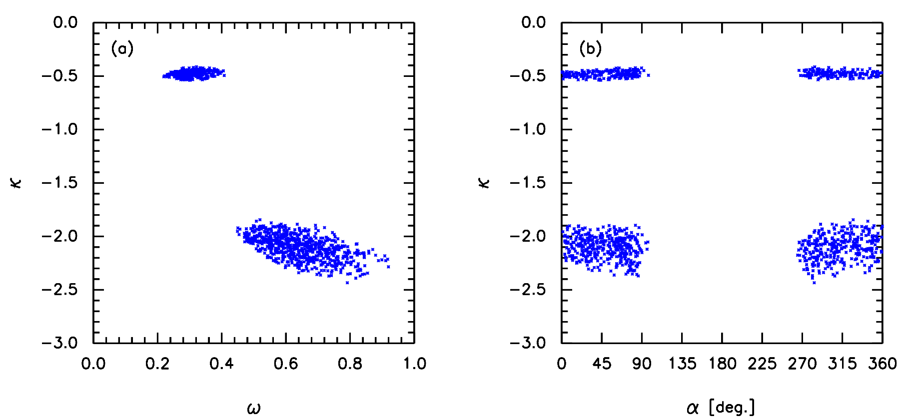

FIG. 2 (color online). Allowed parameter regions by the 3σ experimental constraints in Eq. (17) for Case 3 ($M_1 \gg M_2$) in Eq. (9). Here we take $\eta = 1000$.

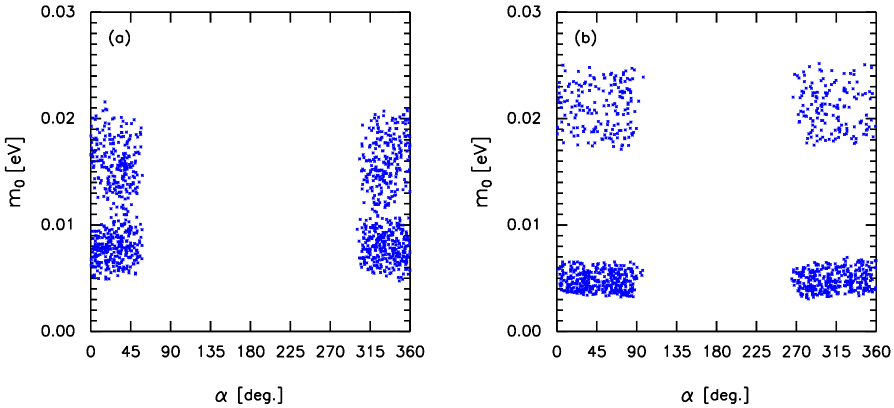

FIG. 3 (color online). Predictions of m_0 over allowed parameter regions by the 3σ experimental constraints in Eq. (17) for (a) Case 2 and (b) Case 3 in Eq. (9).

is satisfied. Because of this condition, it appears that two allowed regions are separated in Fig. 1.

(ii) For Case 3, the expression for θ_{12} is further simplified as

$$\tan 2\theta_{12} \simeq \frac{2\sqrt{2}(1+\kappa)\omega\cos^2\frac{\alpha}{2}\{(1+\kappa)^2 + 2\omega^2\cos\alpha\}}{(1+\kappa)^4 + (\kappa-1)^2\omega^2(\cos\alpha - 1)}. \tag{20}$$

In this case we found that only the parameter regions leading to $|1+\kappa| \geq |\omega|$ are allowed by the result from the solar neutrino experiments.

(iii) For vanishing phase $\alpha = 0$, we can easily see that $\theta_{23} = \frac{\pi}{4}$, $\theta_{13} = 0$ and $\tan 2\theta_{12} = \frac{2\sqrt{2}\omega(1+\kappa)}{(1+\kappa)^2+2\omega^2(\frac{1}{\eta}-1)}$, which can be consistent with the result of the solar neutrino experiments. However, $\alpha = \pi$ is not allowed because it would result in $\theta_{12} = 0$ as can be seen from Eq. (20).

In Fig. 3, we present the prediction of the parameter m_0, which determines the overall mass scale of the light neutrinos, as a function of α for $\eta = 1(1000)$. Combining the allowed regions for the parameters κ and ω shown in Fig. 1 and 2, m_0 in our model is turned out to be of order $10^{-3} \sim 10^{-2}$ eV, which is around the atmospheric scale $m_0 \sim \sqrt{\Delta m^2_{atm}}/2$ as expected from the fact that our scenario is relevant for the normal hierarchical light neutrino mass spectrum.

Next, we consider how our scenario predicts the sizes of θ_{13} and Dirac phase δ. In Fig. 4, we show the predictions of $|U_{e3}|$ as a function of the phase α for Case 2 and Case 3. The horizontal solid (dotted) lines correspond to the experimental bound on θ_{13} from CHOOZ experiment at $3\sigma(2\sigma)$ C.L., respectively. For Case 2, $|U_{e3}|$ is predicted well below the current bound. Thus, the current experimental bound on θ_{13} does not constrain the parameter space. Contrary to Case 2, Fig. 4(b) shows that the experimental bound on θ_{13} can constrain the parameter regions for Case 3. We remark that we have cut the points above the 3σ bound in Fig. 4(b). In the parameter regions leading to

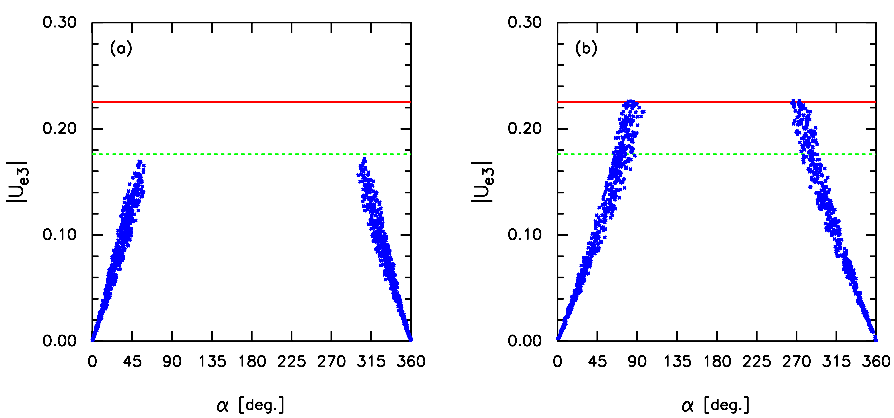

FIG. 4 (color online). Predictions of $|U_{e3}|$ over allowed parameter regions by the 3σ experimental constraints in Eq. (17) for (a) Case 2 and (b) Case 3 in Eq. (9). The horizontal solid (dotted) lines are 3σ (2σ) upper bounds, respectively.

the best-fit points of the neutrino mixing angles, we obtain the following approximate expressions for U_{e3} and the phase angle δ of $U_{\rm PMNS}$:

$$|U_{e3}| \simeq \frac{\omega}{|\kappa - 1|}\sqrt{1-\cos\alpha}, \tag{21}$$

$$\sin\delta \simeq -\cos\frac{\alpha}{2}. \tag{22}$$

Interestingly enough, we see that the nonvanishing $|U_{e3}|$ depends on the nontrivial value of α and it is also related with the phase δ. These approximate expressions are the same as those given in Ref. [14].

The atmospheric mixing angle θ_{23} is also deviated from the maximal mixing. The deviation is approximately given by

$$\theta_{23} - \frac{\pi}{4} \simeq \frac{(1-\kappa^2)}{4\kappa(1+\kappa^2)}\omega^2 \sin^2\frac{\alpha}{2}. \tag{23}$$

We see from the above expression that the atmospheric neutrino mixing goes to maximal for $\alpha = 0$, and the parameter regions consistent with the solar neutrino and CHOOZ experiments indicate that the deviation from maximality of the atmospheric mixing angle so small that it is well below the experimental limit of θ_{23}.

Now let us consider the neutrinoless double beta decay which is related with the absolute value of the ee-element of the light neutrino mass matrix and is approximately given in our scenario by

$$|\langle m_{ee}\rangle| \simeq |m_0(e^{2i\alpha}+1)\omega^2| = m_0\omega^2\sqrt{2(1+\cos 2\alpha)}. \tag{24}$$

As can be seen in the above equation, m_{ee} vanishes for $\alpha = \pi/2$ or $3\pi/2$ in our model. In Fig. 5, we show the predictions for m_{ee} as a function of the phase α. Case 2 predicts larger m_{ee} than Case 3, and even gives lower limits, $m_{ee} > 0.003$ eV.

IV. LEPTOGENESIS

We now consider how leptogenesis can work out in our scenario. For the decay of a heavy Majorana neutrino N_i, the CP asymmetry generated through the interference between tree and one-loop diagrams is given by [19,20]:

$$\text{CP Asymmetry}: \varepsilon_i = \frac{\Gamma(N_i \to l\varphi) - \Gamma(N_i \to \bar{l}\varphi^\dagger)}{\Gamma(N_i \to l\varphi) + \Gamma(N_i \to \bar{l}\varphi^\dagger)} = \frac{1}{8\pi}\sum_{k\neq i}\frac{\mathrm{Im}[Y_\nu Y_\nu^\dagger]_{ik}^2}{(Y_\nu Y_\nu^\dagger)_{ii}}\tilde{f}\left(\frac{M_k^2}{M_i^2}\right),$$

where M_i denotes the heavy Majorana neutrino masses and the loop function $\tilde{f}(x_i)$ containing vertex and self-energy corrections is

$$\tilde{f}(x) = \sqrt{x}\left((1+x)\ln\frac{x}{1+x} + \frac{2-x}{1-x}\right). \tag{25}$$

We note that the asymmetry ε_1 due to the decay of the heavy Majorana neutrino N_1 vanishes because the CP phase does not show up in the relevant terms due to $\rho = 0$:

$$\mathrm{Im}[Y_\nu Y_\nu^\dagger]_{i1}^2 = \mathrm{Im}[Y_\nu Y_\nu^\dagger]_{1i}^2 = 0. \tag{26}$$

In fact, nonvanishing but small $\rho(\equiv a/d)$, whose size is constrained by neutrino data, can lead to nonzero ε_1. However, the numerical value of lepton asymmetry generated from nonvanishing $[Y_\nu Y_\nu^\dagger]_{i1}^2$ is still too small for successful leptogenesis.

Since there are no contributions of N_1 to $\varepsilon_{2(3)}$ due to Eq. (26), the lepton asymmetry can be generated only in case that the degeneracy between N_2 and N_3 is broken. And quasidegeneracy is still desirable because it does not much affect the results for low energy neutrino observables obtained in Sec. III. We find that even a tiny mass splitting between N_2 and N_3 on top of the $\mu - \tau$ symmetry breaking through the Dirac CP phase can lead to successful leptogenesis. We expect that lepton asymmetry is resonantly enhanced in our case [21,22]. For convenience, we intro-

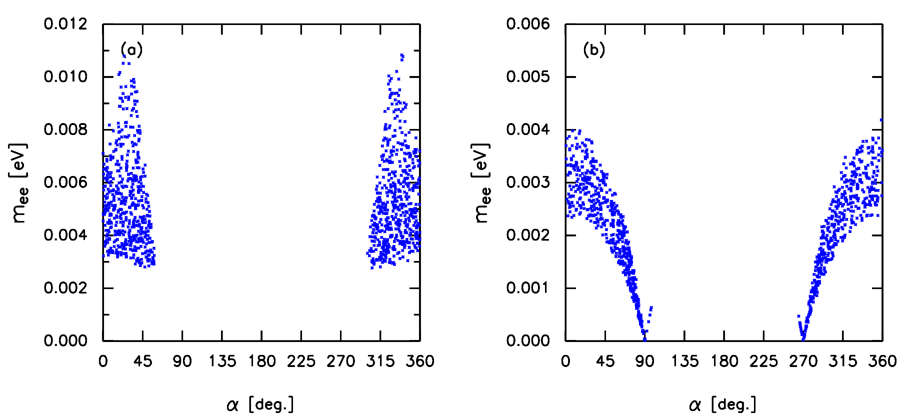

FIG. 5 (color online). Predictions for the effective mass m_{ee} for the neutrinoless double β-decay over allowed parameter regions by the 3σ experimental constraints in Eq. (17) for (a) Case 2 and (b) Case 3 in Eq. (9).

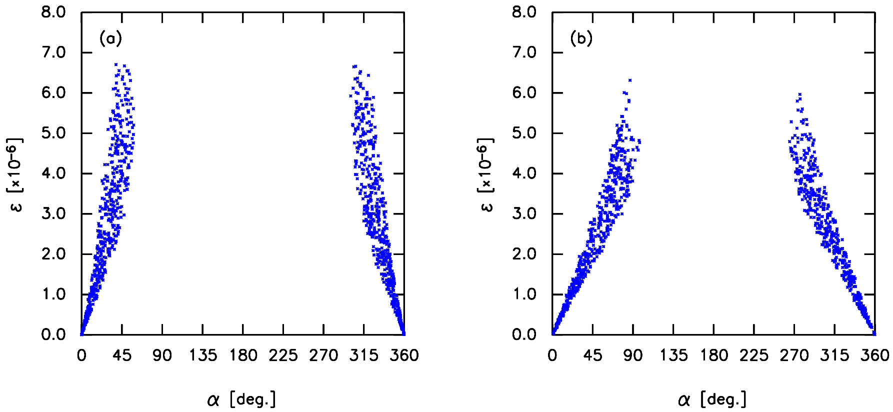

FIG. 6 (color online). Predictions for the CP asymmetry ϵ for resonant leptogenesis over allowed parameter regions by the 3σ experimental constraints in Eq. (17) for (a) Case 2 and (b) Case 3 in Eq. (9). The dependence on d(or M_2) and δ_N is proportional to each other, that is, this figure corresponds to $M_2 = 10^{10}$ (GeV) with $\delta_N = 10^{-2}$ or $M_2 = 10^8$ (GeV) with $\delta_N = 10^{-4}$, etc.

duce a parameter δ_N representing the degree of degeneracy as follows:

$$\delta_N \equiv \frac{M_3 - M_2}{M_2}. \qquad (27)$$

Since δ_N is taken to be very small, the CP asymmetries $\varepsilon_{2(3)}$ are approximately given by

$$\begin{aligned} \varepsilon_2 &\simeq \frac{-1}{16\pi(Y_\nu Y_\nu^\dagger)_{22}}\left\{\frac{\mathrm{Im}[(Y_\nu Y_\nu^\dagger)_{23}^2]}{\delta_N}\right\}, \\ \varepsilon_3 &\simeq \frac{1}{16\pi(Y_\nu Y_\nu^\dagger)_{33}}\left\{\frac{\mathrm{Im}[(Y_\nu Y_\nu^\dagger)_{32}^2]}{\delta_N}\right\}, \end{aligned} \qquad (28)$$

where we have used $\tilde{f}[(1+\delta_N)^{\pm 2}] \simeq \mp(1/2\delta_N)$ for $\delta_N \ll 1$ [22]. The relevant Yukawa terms in our scenario are as follows,

$$\begin{aligned} (Y_\nu Y_\nu^\dagger)_{22(33)} &= d^2(1+\kappa^2+\omega^2), \\ \mathrm{Im}[(Y_\nu Y_\nu^\dagger)_{23}^2] &= -2d^4\omega^2(2\kappa + \omega^2\cos\alpha)\sin\alpha, \\ \mathrm{Im}[(Y_\nu Y_\nu^\dagger)_{32}^2] &= 2d^4\omega^2(2\kappa + \omega^2\cos\alpha)\sin\alpha, \end{aligned} \qquad (29)$$

and then the resulting CP asymmetries are given by

$$\varepsilon_2 = \varepsilon_3 \simeq \frac{1}{8\pi}\frac{d^2\omega^2(2\kappa+\omega^2\cos\alpha)\sin\alpha}{\delta_N(1+\kappa^2+\omega^2)}. \qquad (30)$$

In this expression, the values of the parameters ω, κ, α are determined from the analysis described in Sec. III, whereas δ_N and d are arbitrary. However, since $d^2 = m_0 M_2/v^2$ as defined in Eq. (7), the value of d depends on the magnitude of M_2 in the case that m_0 is determined as before. Thus, in our numerical analysis, we take M_2 and δ_N as input in the estimation of lepton asymmetry. Here, we note that although δ_N and M_2 are taken to be independent parameters in our analysis, the predictions of the lepton asymmetry $\varepsilon_{2(3)}$ depends only on the quantity M_2/δ_N. In Fig. 6, we show the predictions of the total lepton asymmetry for the specific values of δ_N and M_2. It is likely from Eq. (30) that one could arbitrarily enhance the asymmetry by lowering δ_N. However, the value of δ_N is constrained from the validity of the perturbation. In order for the perturbative approach to be valid, the tree-level decay width Γ_i must be much smaller than the mass difference:

$$\Gamma_i = \frac{[Y_\nu Y_\nu^\dagger]_{ii}}{8\pi}M_i \ll M_3 - M_2 = \delta_N M_2, \qquad i = 2, 3. \qquad (31)$$

Numerically, our model requires $\delta_N \gg 10^{-7}$ for $M_2 = 10^{10}$ GeV, and so the maximum degeneracy or the minimum δ_N in our scenario could be

$$\delta_N^{\min} \sim 10^{-6} \times \left(\frac{M_2}{10^{10}\ \mathrm{GeV}}\right). \qquad (32)$$

Now, let us study how we can achieve successful baryon asymmetry in our model. Actually, the resulting baryon-to-photon ratio can be estimated as

$$\eta_B \simeq 10^{-2}\sum_i \varepsilon_i \cdot \kappa_i \qquad (33)$$

where the efficiency factor κ_i describe the washout of the produced lepton asymmetry ε_i. The efficiency in generating the resultant baryon asymmetry is usually controlled by the parameter defined as

$$K_i \equiv \frac{\Gamma_i}{H} = \frac{\tilde{m}_i}{m_*}, \qquad (34)$$

where Γ_i is the tree-level decay width of N_i and H is the Hubble constant. Here, the so-called effective neutrino mass, $\tilde{m}_i$ is

$$\tilde{m}_i = \frac{[m_D m_D^\dagger]_{ii}}{M_i}, \qquad (35)$$

and m_* is defined as

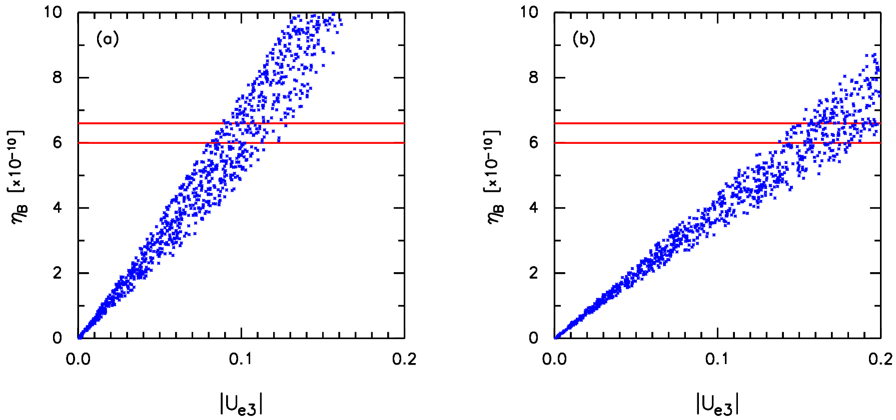

FIG. 7 (color online). Predictions for the baryon asymmetry η_B over $|U_{e3}|$ for (a) Case 2 and (b) Case 3 in Eq. (9). Here we take $\delta_N = 10^{-6}$ and $M_2 = 3 \times 10^6$ (GeV). The two horizontal lines are the current bounds from the CMB observations [25].

$$m_* = \frac{16\pi^{5/2}}{3\sqrt{5}} g_*^{1/2} \frac{v^2}{M_{\text{Planck}}} \simeq 1.08 \times 10^{-3}\ \text{eV}, \tag{36}$$

where we adopted $M_{\text{Planck}} = 1.22 \times 10^{19}$ GeV and the effective number of degrees of freedom $g_* \simeq g_{*\text{SM}} = 106.75$. Although most analyses on baryogenesis via leptogenesis conservatively consider $K_i < 1$, much larger values of K_i, even larger than 10^3, can be tolerated [23]. Using the expression of $\tilde{m}_i$ in terms of our parameters defined above,

$$\tilde{m}_i = m_0(1 + \kappa^2 + \omega^2), \tag{37}$$

we find that our scenario resides in so-called *strong wash-out regime* with

$$20 \lesssim K_i \lesssim 30. \tag{38}$$

So, for numerical calculations, we adopt an approximate expression of the efficiency factor applicable for large K_i [24],

$$\kappa_i \approx \frac{0.3}{K_i(\ln K_i)^{0.6}}. \tag{39}$$

In Fig. 7, we present the predictions for η_B over $|U_{e3}|$ for a sufficient degeneracy, $\delta_N = 10^{-6}$, and rather light $M_2 = 3 \times 10^6$ GeV. The two horizontal lines are the current bounds from the CMB observations [25], $\eta_B^{\text{CMB}} = (6.3 \pm 0.3) \times 10^{-10}$ [26]. As shown in Fig. 7, the current observation of η_B^{CMB} can narrowly constrain the value of $|U_{e3}|$. Combining the results presented in Fig. 4 with those from leptogenesis, we can pin down the *CP* phase α, from which the predictions of m_{ee} and ε are constrained, as can be seen from Fig. 5. For example, if $|U_{e3}|$ is determined to be around $|U_{e3}| \sim 0.1$, the *CP* phase α should be around 45°, which in turn leads to $0.003(0.0025) \leq m_{ee} \leq 0.008(0.0035)$ for Case 2 (3).

V. REMARKS AND CONCLUSIONS

In order to achieve leptogenesis, we have demanded the breaking of degeneracy $M_2 = M_3$ in heavy Majorana mass spectrum. The lift of the degeneracy between N_2 and N_3 leads to the $\mu - \tau$ symmetry breaking in the effective light neutrino mass matrix on top of the breaking due to nontrivial *CP* phase. Although tiny breaking of the $\mu - \tau$ symmetry is enough for successful leptogenesis, its breaking effect may affect our predictions for neutrino masses and mixing described in Sec. III. The most severe influence can be happened in the prediction of nonvanishing θ_{13}. So, let us estimate how much it can be affected by δ_N demanded for successful leptogenesis. Taking $M_N = \text{Diag}[M_1, M_2, M_3]$ and imposing $\alpha = 0$ in Eq. (3), we obtain

$$\theta_{13} \simeq \frac{\omega(\kappa - 1)}{\sqrt{2}(\omega^2 - \frac{(\kappa-1)^2}{2})} \frac{M_3 - M_2}{M_3 + M_2}. \tag{40}$$

Using the allowed regions of the parameters κ and ω shown in in Figs. 1 and 2, we estimate that

$$\theta_{13} < 0.2\delta_N. \tag{41}$$

So, we find that the θ_{13} generated by the generic $\mu - \tau$ symmetry breaking is less than 0.2° even for $\delta_N = 10^{-2}$, which does not hurt the analysis for the neutrino masses and mixing described in Sec. III. Although the mass splitting δ_N and the phase angle α are totally independent in our consideration, both can generate the nonzero θ_{13} as shown in Eqs. (21) and (40). However, as explained above and in Fig. 4, the allowed ranges of the parameter space are quite different, i. e $\theta_{13} < 13°$ from α and $\theta_{13} \sim 0°$ from δ_N.

Finding nonvanishing but small mixing element U_{e3} would be very important in the near future mainly because of completeness of neutrino mixing and possible existence of leptonic *CP* violation. Theoretically, nonvanishing U_{e3} may be related with a certain flavor symmetry breaking in the neutrino sector. In this paper, we proposed a new scenario to break the $\mu - \tau$ symmetry so as to accommodate the nonvanishing U_{e3} while keeping maximal mixing for atmospheric neutrinos. Our scenario is constructed in the context of a seesaw model, and the symmetry breaking is achieved by introducing a *CP* phase in the Dirac Yukawa matrix. Then, the resultant effective light neutrino mass matrix generated through seesaw mechanism reflects the $\mu - \tau$ symmetry breaking which is parameterized in terms of the *CP* phase, and the $\mu - \tau$ symmetry is recovered in the limit of vanishing *CP* phase. We discussed how neutrino mixings and the neutrino mass-squared differences can be predicted and showed how the deviation of θ_{23} from the maximal mixing and nonvanishing U_{e3} depends on the *CP* phase in our scenario.

The prediction for the amplitude in neutrinoless double beta decay has been also studied. However, the Dirac *CP* phase introduced to break the $\mu - \tau$ symmetry does not lead to successful leptogenesis. We found that a tiny breaking of the degeneracy between two heavy Majorana neutrinos on top of the $\mu - \tau$ symmetry breaking through the *CP* phase can lead to successful leptogenesis without much changing the results for the low energy neutrino observables. We also examined how leptogenesis can successfully work out and be related with low energy neutrino measurement in our scenario, and showed that our predictions for the neutrino mixing can be severely constrained by the current observation of baryon asymmetry. Future measurement for U_{e3} would play an important role of test of our scenario and provide us with some indication on baryon asymmetry in our Universe.

ACKNOWLEDGMENTS

Y. H. A was supported in part by Brain Korea 21 Program and in part by CHEP-SRC Program and in part by the Korea Research Foundation Grant funded by the Korean Government (MOEHRD) No. KRF-2005-070-C00030. C. S. K was supported by the Korea Research Foundation Grant funded by the Korean Government (MOEHRD) No. R02-2003-000-10050-0. J. L was supported in part by Brain Korea 21 Program and in part by Grant No. F01-2004-000-10292-0 of KOSEF-NSFC International Collaborative Research Grant. S. K. K and J. L were supported in part by the SRC program of KOSEF through CQUeST with Grant No. R11-2005-021.

[1] Y. Fukuda *et al.* (Super-Kamiokande Collaboration), Phys. Rev. Lett. **81**, 1562 (1998).

[2] S. Hukuda *et al.* (Super-Kamiokande Collab.), Phys. Rev. Lett. **86**, 5656 (2001); Phys. Lett. B **539**, 179 (2002).

[3] Q. Ahmad *et al.* (SNO Collab.), Phys. Rev. Lett. **87**, 071301 (2001); (), Phys. Rev. Lett. **89**, 011301 (2002); (), Phys. Rev. Lett. **92**, 181301 (2004).

[4] M. Apollonio *et al.* (CHOOZ Collaboration), Phys. Lett. B **420**, 397 (1998).

[5] E. Ma and G. Rajasekaran, Phys. Rev. D **64**, 113012 (2001); E. Ma, Mod. Phys. Lett. A **17**, 627 (2002); **17**2361 (2002); Phys. Rev. D **70**, 031901 (2004); S. -L. Chen, M. Frigerio, and E. Ma, Phys. Rev. D **70**, 073008 (2004).

[6] K. S. Babu, E. Ma, and J. W. F. Valle, Phys. Lett. B **552**, 207 (2003); J. Kubo, A. Mondragon, M. Mondragon, and E. Rodriguez-Jauregui, Prog. Theor. Phys. **109**, 795 (2003); J. Kubo, Phys. Lett. B **578**, 156 (2004); Q. Shafi and Z. Tavartkiladze, Phys. Lett. B **594**, 177 (2004); Phys. Lett. B **633**, 595 (2006); M. Frigerio, S. Kaneko, E. Ma, and M. Tanimoto, Phys. Rev. D **71**, 011901 (2005).

[7] S. K. Kang and C. S. Kim, Phys. Lett. B **634**, 520 (2006); S. K. Kang, Z.-z. Xing, and S. Zhou, Phys. Rev. D **73**, 013001 (2006).

[8] T. Fukuyama and H. Nishura, hep-ph/9702253; R. N. Mohapatra and S. Nussinov, Phys. Rev. D **60**, 013002 (1999); H. Nishiura, K. Matsuda, and T. Fukuyama, Phys. Rev. D **60**, 013006 (1999); K. Matsuda, T. Fukuyama, and H. Nishiura, Phys. Rev. D **61**, 053001 (2000); E. Ma and M. Raidal, Phys. Rev. Lett. **87**, 011802 (2001); A. Datta and P. J. O'Donnell, Phys. Rev. D**72**, 113002 (2005); K. R. S. Balaji, W. Grimus, and T. Schwetz, Phys. Lett. B **508**, 301 (2001); P. F. Harrison and W. G. Scott, Phys. Lett. B **547**, 219 (2002); E. Ma, Phys. Rev. D **66**, 117301 (2002); Y. Koide *et al.*, Phys. Rev. D **66**, 093006 (2002); K. Matsuda and H. Nishiura, Phys. Rev. D **69**, 053005 (2004); hep-ph/051133; Y. Koide, Phys. Rev. D **69**, 093001 (2004); A. Ghosal, Mod. Phys. Lett. A **19**, 2579 (2004); C. S. Lam, Phys. Lett. B **507**, 214 (2001); Phys. Rev. D **71**, 093001 (2005); S. Choubey and W. Rodejohann, Eur. Phys. J. C **40**, 259 (2005).

[9] T. Kitabayashi and M. Yasuè, Phys. Lett. B **524**, 308 (2002); Int. J. Mod. Phys. A **17**, 2519 (2002); Phys. Rev. D **67**, 015006 (2003); I. Aizawa, M. Ishiguro, T. Kitabayashi, and M. Yasuè, Phys. Rev. D **70**, 015011 (2004); I. Aizawa, T. Kitabayashi, and M. Yasuè, Phys. Rev. D **71**, 075011 (2005); T. Kitabayashi and M. Yasue, Phys. Lett. B **621**, 133 (2005); I. Aizawa and M. Yasue, Phys. Rev. D **73**, 015002 (2006); I. Aizawa, T. Kitabayashi, and M. Yasue, Nucl. Phys. **B728**, 220 (2005).

[10] W. Grimus and L. Lavoura, J. High Energy Phys. 07 (2001) 045; Eur. Phys. J. C **28**, 123 (2003); Phys. Lett. B **572**, 189 (2003); Phys. Lett. B **579**, 113 (2004); J. Phys. G **30**, 1073 (2004); J. High Energy Phys. 08 (2005) 013; J. High Energy Phys. 08 (2005) 013; W. Grimus, A. S. Joshipura, S. Kaneko, L. Lavoura, and M. Tanimoto, J. High Energy Phys. 07 (2004) 078; W. Grimus, A. S. Joshipura, S. Kaneko, L. Lavoura, H. Sawanaka, and M. Tanimoto, Nucl. Phys. **B713**, 151 (2005); M. Tanimoto, hep-ph/0505031; W. Grimus, S. Kaneko, L. Lavoura, H. Sawanaka, and M. Tanimoto, J. High Energy Phys. 01 (2006) 110; A. S. Joshipura, hep-ph/0512252.

[11] R. N. Mohapatra, J. High Energy Phys. 10 (2004) 027; R. N. Mohapatra and S. Nasri, Phys. Rev. D **71**, 033001

(2005); R. N. Mohapatra, S. Nasri, and Hai-Bo Yu, Phys. Lett. B **615**, 231 (2005); Phys. Rev. D **72**, 033007 (2005).

[12] S. M. Barr and I. Dorsner, Nucl. Phys. **B585**, 79 (2000); W. J. Marciano, hep-ph/0108181; O. L. G. Peres and A. Yu. Smirnov, Nucl. Phys. **B680**, 479 (2004); Nucl. Phys. B, Proc. Suppl. **110**, 355 (2002); A. S. Joshipura, hep-ph/0411154.

[13] Y. Itow *et al.*, hep-ex/0106019.

[14] R. N. Mohapatra and W. Rodejohann, Phys. Rev. D **72**, 053001 (2005).

[15] S. F. King, J. High Energy Phys. 09 (2002) 011.

[16] P. F. Harrison, D. H. Perkins, and W. G. Scott, Phys. Lett. B **530**, 167 (2002).

[17] I. Aizawa and M. Yasuè, Phys. Lett. B **607**, 267 (2005).

[18] M. Maltoni, T. Schwetz, M. A. Tortola, and J. W. F. Valle, New J. Phys. **6**, 122 (2004); .more updated bounds can be found in the latest version of New J. Phys.**6**, 122 (2004).

[19] M. Fukugita and T. Yanagida, Phys. Lett. B **174**, 45 (1986).

[20] L. Covi, E. Roulet, and F. Vissani, Phys. Lett. B **384**, 169 (1996); W. Buchmüller and M. Plümacher, *ibid.* **431**, 354 (1998).

[21] M. Flanz, E. A. Paschos, and U. Sarkar, Phys. Lett. B **345**, 248 (1995); A. Pilaftsis, Phys. Rev. D **56**, 5431 (1997); W. Buchmüller and M. Plümacher, Phys. Lett. B **431**, 354 (1998); A. Pilaftsis, Int. J. Mod. Phys. A **14**, 1811 (1999).

[22] G. C. Branco, R. González Felipe, F. R. Joaquim, I. Masina, M. N. Rebelo, and C. A. Savoy, Phys. Rev. D **67**, 073025 (2003).

[23] A. Pilaftsis and T. E. J. Underwood, Nucl. Phys. **B692**, 303 (2004); Phys. Rev. D **72**, 113001 (2005).

[24] H. B. Nielsen and Y. Takanishi, Phys. Lett. B **507**, 241 (2001).

[25] D. N. Spergel *et al.* (WMAP Collaboration), Astrophys. J. Suppl. Ser. **148**, 175 (2003); M. Tegmark *et al.*, Phys. Rev. D **69**, 103501 (2004).

[26] W. Buchmuller, P. Di Bari, and M. Plumacher, Ann. Phys. **315**, 305 (2005).